Journal of Materials Chemistry A

PAPER

View Article Online
View Journal | View Issue

Cite this: J. Mater. Chem. A, 2016, 4, 3886

Highly stable poly(ethylene glycol)-grafted alkaline anion exchange membranes†

Congrong Yang,[ab] Suli Wang,[a] Wenjia Ma,[a] Shixiong Zhao,[a] Ziqi Xu[c] and Gongquan Sun*[a]

Received 8th January 2016
Accepted 4th February 2016

DOI: 10.1039/c6ta00200e

www.rsc.org/MaterialsA

A mechanically and chemically stable poly(ethylene glycol) (PEG)-grafted poly(styrene-ethylene-*co*-butylene-styrene) (SEBS)-based alkaline anion exchange membrane (AAEM) was designed, prepared and characterized. When subjected to tensile strain, the elongation at breaking of these SEBS-based AAEMs was up to 500%, a value 80 times greater than that of an AAEM using polystyrene as the main chain. Remarkably, the ion exchange capacity (IEC), conductivity, dimensions and mechanical properties of this AAEM could remain almost unchanged in 2.5 M KOH at 60 °C for about 3000 h, indicating the excellent alkaline stability of the PEG-grafted SEBS-based AAEMs. As confirmed by TEM, the grafting of PEG could enlarge the size of the ion-conducting channels, significantly enhancing the conductivity of these AAEMs (80 °C, from 29.2 mS cm^{-1} to 51.9 mS cm^{-1}). Furthermore, the peak power density of an H_2/O_2 single fuel cell using this SEBS-based AAEM was up to 146 mW cm^{-2} at 50 °C. Based on these outstanding properties, this membrane has potential application not only for fuel cells, but also for other electrochemical energy conversion and storage devices, such as redox flow and alkaline ion batteries.

Introduction

Favoring the use of non-precious metal catalysts, alkaline anion exchange membranes (AAEMs) have evoked great interest in many electrochemical energy systems, such as fuel cells,[1–3] flow[4,5] and metal/air batteries,[6] electrolyzers,[7,8] reverse electrodialysis cells[9] and bioelectrochemical systems.[10] For the application in the above systems, the AAEMs should possess good physical and chemical properties (not only high ionic conductivity and good mechanical strength but also high chemical stability). In the past decades, great efforts have been devoted to enhancing the performance of AAEMs to meet the requirement of these electrochemical systems. However, it is not easy to prepare an AAEM that could fulfill all of these requirements. Two main disadvantages — their relatively poor chemical stability and low ion conductivity (especially when the AAEM is not fully hydrated) — of AAEMs restrict their widespread application. To date, the conductivity of the AAEM has been greatly improved (more than 0.1 S cm^{-1} at 80 °C) with the efforts of various researchers.[11,12] Therefore, in the severe alkaline environment in which they must operate due to the presence of OH^- (a strong nucleophilic ion), the chemical stability of AAEMs is still considered to be a primary and tough challenge.[13,14] Though lifetime studies indicate that the cation stability is of paramount importance for the stable operation of AAEMs,[12,15–29] recent study results have shown that equally important is the stability of the polyaromatic backbone under high pH conditions. It has been proved that the aromatic containing ether-based main chain would be severely degraded *via* ether hydrolysis and/or quaternary carbon hydrolysis in the alkaline solution at 60 °C.[30,31] Therefore, a stable polymer main chain is also greatly important for the improvement of AAEMs.

According to our previous work, the polystyrene main chain has been proved to possess better alkaline stability than that of poly(2,6-dimethyl-1,4-phenylene oxide) (PPO), polysulfone and other aromatic containing ether main chains, which has also been found by other groups.[28] However, the poor mechanical stability (especially when AAEMs are in the dry condition) of AAEMs based on polystyrene (a rigid polymer) is a challenge for the application of this membrane.

In order to achieve a mechanically and chemically stable AAEM, poly(styrene-ethylene-*co*-butylene-styrene) (SEBS) with good flexibility is selected as the main chain of the AAEMs in this work. To further enhance the conductivities of the SEBS-based AAEMs, effective ion-conducting channels were constructed in the AAEMs by grafting poly(ethylene glycol) (PEG) onto the SEBS main chain. The influences of the degree of chloromethylation of SEBS and the grafting state of PEG (molecular weight and graft degree) on the morphology and the

[a]Division of Fuel Cell & Battery, Dalian National Laboratory for Clean Energy, Dalian Institute of Chemical Physics, Chinese Academy of Sciences, 457 Zhongshan Road, Dalian 116023, PR China. E-mail: gqsun@dicp.ac.cn; Tel: +86-411-84379063

[b]University of the Chinese Academy of Sciences, Beijing 100039, PR China

[c]Dalian University of Technology, Dalian 116023, PR China

† Electronic supplementary information (ESI) available: ^{1}H NMR spectra of SEBS, CMSEBS and SEBS$_x$-*g*-PEG$_y$-*M*, alkaline stability of QA-SEBS$_{0.15}$-*g*-PEG$_y$-1000, some explanation for the performance of the fuel cell using SEBS-based AAEM. See DOI: 10.1039/c6ta00200e

physical and chemical properties (such as IEC, water uptake, degree of swelling and ionic conductivity) are then investigated in detail.

Experimental section

Materials

SEBS 6152 (molecular weight of 70 000, 27% styrene content) was obtained from Taipol company. 1,4-Bis(chloromethoxyl) butane (BCMB) was from Langene bio-science Co., Ltd. Anhydrous tin chloride, poly(ethylene glycol) monomethyl ether (MPEG) (350, 750 and 1000), sodium hydride (60% w/w in mineral oil) and trimethylamine aqueous solution were purchased from Aladdin Industrial Inc.

Preparation of poly(ethylene glycol) grafted SEBS-based AAEMs

To obtain a highly stable and conductive AAEM, the molecular structure of the polymer used for preparing the AAEMs was designed as shown in Fig. 1. SEBS, the main chain, possesses good flexibility and good chemical stability in alkaline conditions, which is suitable for AAEMs. The processes for the poly(ethylene glycol) grafted SEBS-based AAEMs include chloromethylation, PEG-grafting and quaternization. The synthetic routes are shown in Scheme 1. The chloromethylation of SEBS and PEG-grafting were considered to be two rather important processes that determined the properties of the PEG-grafted SEBS-based AAEMs. Therefore, the influence of CD, PEG-grafting degree and the molecular weight of PEG on the microstructure and the properties of the AAEMs were investigated in detail.

Chloromethylation of SEBS

The chloromethylation of SEBS was achieved by the reaction of SEBS polymer and BCMB catalyzed by anhydrous tin chloride. The chloromethylation degree of SEBS could be effectively modulated by controlling the reaction temperature and reaction time. The procedure was as follows: SEBS (2 g) was dissolved in CCl_4 (30 mL) at 40 °C. Anhydrous tin chloride (0.5 mL) was added into the solution at 5 °C, followed by the dropwise addition of BCMB (3 mL). The mixture was stirred below 20 °C for a period of time and poured into ethanol to precipitate the product. The crude product was dissolved in THF and then precipitated again by ethanol. After being washed several times with ethanol and water, the product was dried under vacuum at room temperature.

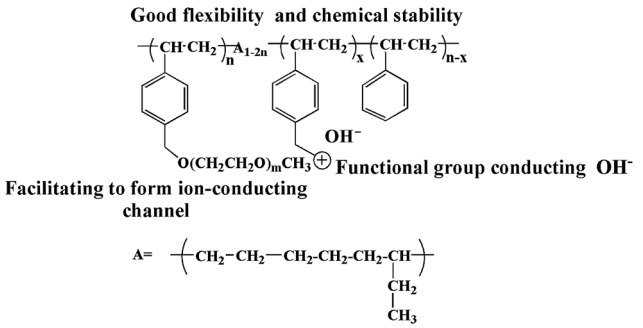

Fig. 1 Molecular structure of the designed polymer for the preparation of AAEMs.

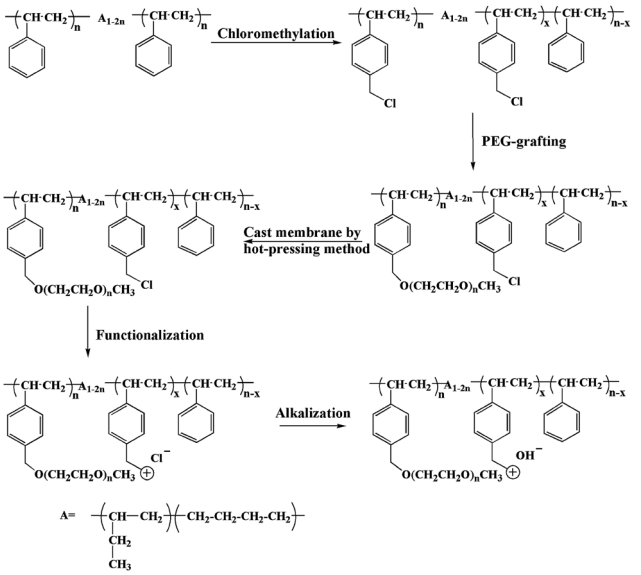

Scheme 1 Synthetic routes of poly(ethylene glycol)-grafted SEBS-based AAEMs.

Preparation of PEG-grafted SEBS-based membranes

The grafting of PEG onto the SEBS main chain was achieved by the reaction of SEBS chloride and poly(ethylene glycol) monomethyl ether (MPEG). The above synthesized SEBS chloride was dissolved in THF (3% w/v). A certain amount of MPEG was added into the solution and NaH was slowly added. The mixture was allowed to react at 40 °C for 14 h. Then it was poured into ethanol to obtain a light yellow and slightly transparent solid. The product was dried under vacuum at 30 °C. Finally, the PEG-grafted SEBS-based membranes were prepared by the hot-pressed method with 20 000 pounds pressure at 120 °C.

Quaternization of PEG-grafted SEBS-based membranes

The above prepared membranes were quaternized by immersing them in trimethylamine aqueous solution at room temperature for 24 h. The membranes could be changed into OH^- form *via* treating them in in their Cl^- form in 1 M KOH solution at room temperature for two days. The membranes were denoted as QA-SEBS$_x$-*g*-PEG$_y$-*M* (QA is quaternary ammoniums, x is chloromethylation degree (CD), y is PEG-grafting degree and M is the molecular weight of MPEG).

NMR spectra

^{1}H NMR spectra were recorded on a Bruker ACIII 400 spectrometer. CD of SEBS and PEG-grafting degree (x and y) could be calculated by the relative integrated intensities of the ^{1}H resonances (as shown in Fig. S1,† $CDCl_3$ as solvent).

Morphological characterization

The morphologies of the membranes were characterized by transmission electron microscopy (TEM) using a JEM-2100 microscope operating at an accelerating voltage of 200 kV. TEM sections were prepared using an ultracryomicrotome. For observation, these samples were stained by exposure to H_2PtCl_6 (in ethylene glycol). The TEM data represent partially hydrated films that have been equilibrated under ambient conditions.

Ionic conductivity of the membranes

The resistance values of the AAEMs were measured over the frequency range from 1 Hz to 1 MHz by alternating current (ac) impedance spectroscopy, using an electrode system connected with a Solartron 1287 electrochemical workstation and a Solartron 1260 gain-phase analyzer. All samples were placed in deionized water and equilibrated for at least 30 min at a given temperature. The membranes were repeatedly conducted three times.

The in-plane conductivity was calculated as follows:

$$\sigma = \frac{L}{WTR}$$

where σ is the conductivity of the membrane in S cm^{-1}, L is the length of the membrane between sensor II and reference electrodes in cm, W and T are the width and thickness of the membrane in cm, respectively. R is the resistance of the membrane in ohms.

Ion exchange capacity (IEC), water uptake (WU), swelling degree (SD) and absorbed water capacity (λ) of the membranes

The IEC of the AAEMs was determined by the back-titration method. The AAEMs in OH-form were immersed in 10 mL 0.01 mol L^{-1} HCl solution for two days. Then the solutions were titrated with 0.01 M KOH solution using a pH meter to determine the titration-end point. IEC values were calculated using the following expression:

$$\mathrm{IEC}(\mathrm{mmol\ g^{-1}}) = \frac{V_{0\mathrm{KOH}} C_{\mathrm{KOH}} - V_{\mathrm{iKOH}} C_{\mathrm{KOH}}}{m_{\mathrm{dry}}} \times 1000$$

where $V_{0\mathrm{KOH}}$ and V_{iKOH} are the volumes of the KOH consumed in the titration without and with membranes, respectively, C_{KOH} was the molar concentration of KOH, and m_{dry} is the mass of the dried membrane in OH^- form.

The WU and the SD of the membranes in OH^- form are calculated from the weight and dimension differences of membranes after soaking in deionized water for 48 h at room temperature and after drying in a vacuum oven at 60 °C.

The WU is calculated by the equation as follows:

$$\mathrm{WU}(\%) = \frac{W_{\mathrm{wet}} - W_{\mathrm{dry}}}{W_{\mathrm{dry}}} \times 100$$

where W_{wet} and W_{dry} are the weight of wet and dry membranes in OH^- forms in grams, respectively.

The SD was calculated by the equation as follows:

$$\mathrm{SD}(\%) = \frac{L_{\mathrm{wet}} - L_{\mathrm{dry}}}{L_{\mathrm{dry}}} \times 100$$

where L_{wet} and L_{dry} are the geometric width of the wet and dry membranes in OH^- forms, respectively.

The number of absorbed water molecules per functional group, λ, was calculated using the following equation:

$$\lambda = \frac{\mathrm{WU}}{M_{\mathrm{H_2O}} \times \mathrm{IEC}} \times 10$$

Thermomechanical stability of AAEMs

The thermomechanical performances of the grafted SEBS-based AAEMs were tested by DMA using a Q800 dynamic mechanical analyzer from TA Instruments in the stretching mode. The samples were heated from 100 to 300 °C at a heating rate of 3 °C min^{-1} under a dry air atmosphere. A frequency of 1 Hz and a displacement amplitude of 30 μm were used in all DMA measurements.

Alkaline stability of AAEMs

The alkaline stability of the membranes was monitored by measuring the changes of the ionic conductivity, dimensions and IEC values of the membrane before and after being immersed in 2.5 M KOH solution at 60 °C. Prior to testing the conductivity, dimensions and IEC, the membranes were thoroughly washed with deionized water until the conductivity of the water used for washing the membranes was 1.86 μS cm^{-1}.

Single cell tests

The single cell was fabricated by using 70 wt% Pt/C (Johnson Matthey) with a metal loading of 0.5 mg cm^{-2} as both anode and cathode catalysts. Quaternized polystyrene polymer was used as the ionomer with a 20% loading at both electrodes. Then the catalyst ink was sprayed onto the AAEMs to obtain catalyst-coated membranes (CCMs). The membrane electrode assemblies (MEAs) were prepared by hot-pressing the CCM between two gas diffusion layers (GDLs). The MEA in which the ionomer was in OH form was prepared by immersing the above prepared MEA in 1 M KOH solution at room temperature for 48 h. Before being tested, this MEA was thoroughly washed with deionized water. Cells with a 5 cm^2 active area were assembled using stainless steel end-plates. Fuel cell tests were carried out with H_2 and O_2 at 50 °C with 100% relative humidity (RH). The flow rates of H_2 and O_2 were 100 and 200 mL min^{-1} with a 0.2 MPa backpressure, respectively. The MEAs were activated by operating at the constant current densities (100, 200 and 300 mA cm^{-2}). After the activation, the fuel cell polarization curve was measured under dynamic current mode. The cell voltage as a function of current density was recorded using fuel cell testing software.

Results and discussion

Conductivities of PEG-grafted SEBS-based AAEMs

The conductivities of QA-SEBS$_x$-*g*-PEG$_y$-*M* would be significantly influenced by the CD of SEBS, the PEG molecular weight and the PEG-grafting degree (as shown in Fig. 2). From Fig. 2A, it can be

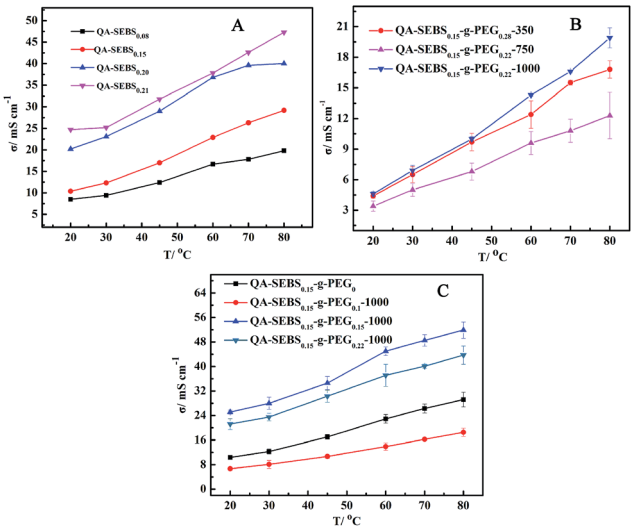

Fig. 2 Conductivities of QA-SEBS$_x$-*g*-PEG$_y$-*M* as a function of temperature: (A) different CD; (B) different molecular weight of PEG; (C) different PEG-grafting degree.

seen that when the CD increases from 0.15 to 0.21, the conductivities of the AAEMs in OH form without PEG-grafting would increase from 10 mS cm^{-1} to 24.7 mS cm^{-1} (room temperature), which is due to the increase of the functional degree. To further investigate the influence of the PEG molecular weight and PEG-grafting degree, the CD was fixed at 0.15. By modulating the PEG molecular weight and PEG-grafting degree, the performance of this AAEM was further optimized. From Fig. 2B, it can be seen that the membrane with a PEG molecular weight of 1000 shows a higher conductivity than that of the membranes with PEG molecular weights of 350 and 750. Then the properties of the membranes with a PEG molecular weight of 1000 were investigated by modulating the PEG-grafting degree. From Fig. 2C, it can be found that the conductivities of the membranes were significantly influenced by the PEG-grafting degree, increasing from 29.2 mS cm^{-1} to 51.9 mS cm^{-1} at 80 °C when the PEG-grafting degree increased to 0.15, and then decreasing to 43.7 mS cm^{-1} when the PEG-grafting degree was 0.22.

IEC, WU, SD and λ of the membranes

Table 1 shows the IEC, WU, SD, and λ of the QA-SEBS$_{0.15}$-*g*-PEG$_y$-1000 membranes. The IEC values of the membranes decreased from 0.75 mmol g^{-1} to 0.42 mmol g^{-1} with the increase of PEG-grafting degree, which is due to the decrease of functional groups and the increase in the molecular weight of the polymers. The SD values of these membranes (from 13.5% to 4.2%) are equal to or even lower than those of the AAEMs with same functional groups (~10%), showing a good dimension stability, especially in the case of the QA-SEBS$_{0.15}$-*g*-PEG$_{0.15}$-1000 membrane. The WU or SD values of the SEBS-based AAEMs with or without PEG-grafting were approximately the same, indicating that the introduction of PEG did not evidently change the water-absorption ability or dimensional stability of the membranes.

Table 1 IEC, WU, SD and λ of the QA-SEBS$_{0.15}$-PEG$_y$-1000 membranes (*y* is 0, 0.1, 0.15 or 0.22)

AAEMs	IEC/mmol g^{-1}	SD/%	WU/%	λ
QA-SEBS$_{0.15}$-PEG$_0$-1000	0.75	10.3 ± 0.64	5.6 ± 0.1	4.1
QA-SEBS$_{0.15}$-PEG$_{0.1}$-1000	0.49	13.5 ± 2.41	4.2 ± 0.5	4.7
QA-SEBS$_{0.15}$-PEG$_{0.15}$-1000	0.47	4.2 ± 0.36	4.2 ± 0.7	5.0
QA-SEBS$_{0.15}$-PEG$_{0.22}$-1000	0.42	9.9 ± 1.13	3.8 ± 1.1	5.0

From the conductivity and the IEC results of these SEBS-based AAEMs, it can be found that the QA-SEBS$_{0.15}$-*g*-PEG$_{0.15}$-1000 membrane shows a relatively lower IEC value but a higher conductivity. This result is opposite to that which we would theoretically expect. What are the factors which lead to the better performance of the QA-SEBS$_{0.15}$-*g*-PEG$_{0.15}$-1000 membrane? To investigate this question, the micro-phase morphologies of these membranes were deeply investigated by TEM.

The effect of the microscale morphology on the physicochemical properties of the membranes

Visually, the prepared membranes are transparent, rather flexible, and can be cut into any size or bent at any angle. The TEM images of the QA-SEBS$_{0.15}$-*g*-PEG$_y$-1000 membranes are shown in Fig. 3. The dark strips shown in TEM are the hydrophilic regions of the QA-SEBS$_{0.15}$-*g*-PEG$_y$-1000 membranes. Using the tri-block copolymer, SEBS, as the main chain, the AAEMs would exhibit a certain degree of hydrophilic/hydrophobic micro-phase separation structure even if there is no PEG-grafting onto

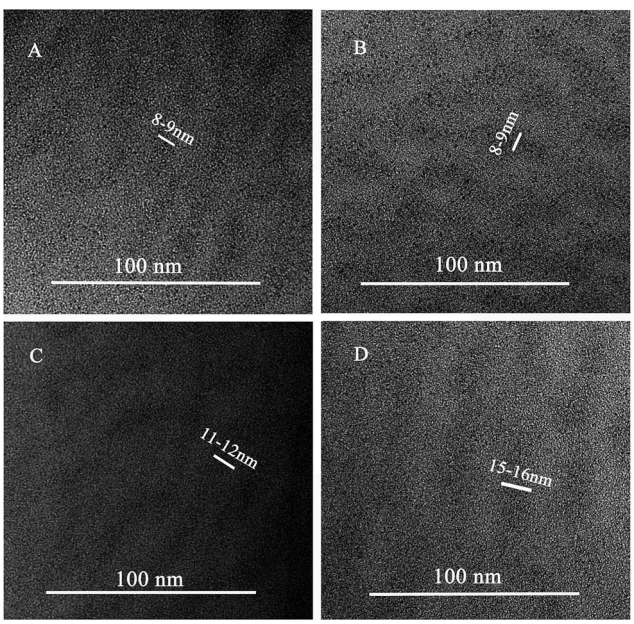

Fig. 3 TEM images of $PtCl_6^{2-}$-stained membranes: (A) QA-SEBS$_{0.15}$-*g*-PEG$_0$; (B) QA-SEBS$_{0.15}$-*g*-PEG$_{0.1}$-1000; (C) QA-SEBS$_{0.15}$-*g*-PEG$_{0.15}$-1000; (D) QA-SEBS$_{0.15}$-*g*-PEG$_{0.22}$-1000.

the main chain. Therefore, the morphologies of the AAEMs with or without PEG-grafting would not show any obvious differences from a visual observation. However, the size of hydrophilic-phase is significantly influenced by the PEG-grafting degree. The average sizes of these regions in QA-SEBS$_{0.15}$-*g*-PEG$_0$, QA-SEBS$_{0.15}$-*g*-PEG$_{0.1}$-1000, QA-SEBS$_{0.15}$-*g*-PEG$_{0.15}$-1000 and QA-SEBS$_{0.15}$-*g*-PEG$_{0.22}$-1000 are 8–9 nm, 8–9 nm, 11–12 nm and 15–16 nm, respectively. So it can be concluded that the increasing of PEG-grafting onto the SEBS main chain will enlarge the size of the ion-conducting channel in the AAEM. The enlarged ion-conducting channel would enhance the conduction of OH^-, so QA-SEBS$_{0.15}$-*g*-PEG$_{0.15}$-1000 shows a higher conductivity. However, the degradation of the IEC, resulting from the larger PEG-grafting degree, would result in a lower conductivity, and the conductivity of QA-SEBS$_{0.15}$-*g*-PEG$_{0.22}$-1000 decreases. Therefore, overall the QA-SEBS$_{0.15}$-*g*-PEG$_{0.15}$-1000 membrane shows the highest conductivity.

Mechanical and thermomechanical stability of the membranes

The SEBS-based AAEMs, which were not easily broken in the tensile testing conditions, possessed super mechanical stability, especially the flexible stability at room temperature (as shown in Fig. 4). From Fig. 4, it can be concluded that the tensile strength (15.5 MPa) and the elongation at break (250%) values of the SEBS-based AAEMs are much higher than those of the polystyrene-based AAEM (11.5 MPa, 6.2%), indicating that the SEBS-based AAEM possesses relatively good toughness and flexibility. Furthermore, the flexibility of the membranes (with elongation at break of up to 500% or even not fractured) was significantly enhanced by grafting PEG onto the SEBS main chain. The dynamic thermomechanical properties of the membranes were investigated by DMA.

The storage modulus E' and the damping values tan δ as a function of temperature are shown in Fig. 5. In general, the

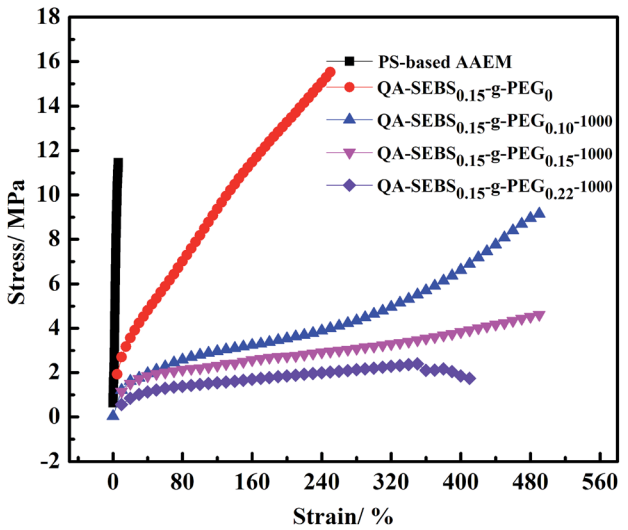

Fig. 4 Mechanical stability curves of AAEMs with polystyrene or SEBS as the main chain.

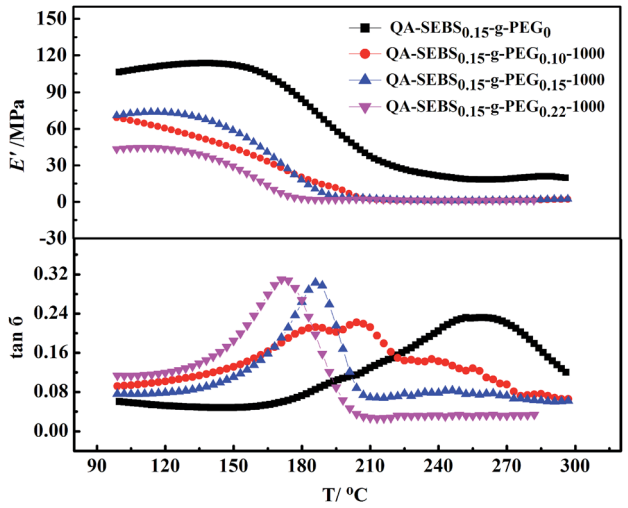

Fig. 5 Storage modulus E' and the damping values tan δ of QA-SEBS$_{0.15}$-*g*-PEG$_y$-1000 as a function of temperature.

α-relaxation processes (reflected by the value of tan δ as a function of temperature) are related to the glass transition temperature, T_g, of the respective membranes. From the DMA test results, it can be seen that PEG-grafting decreases T_g of the membranes (from 258 °C to 170 °C) and the grafting degree did have a significant effect on T_g of the membranes. Furthermore, T_g of these membranes are all higher than 170 °C. The E' values of these AAEMs decreased as the amount of PEG grafted onto the SEBS main chain increased, indicating that the grafting of PEG onto the main chain decreases the toughness of the membranes to a certain degree. From the tensile test and DMA test results, it can be concluded that the mechanical strength and thermal performance of these membranes are relatively good, and could meet the requirements of alkaline electrochemical system working conditions (<100 °C), showing the potential application of these materials in such electrochemical systems, *e.g.* fuel cells.

Alkaline stability of AAEMs

The alkaline stability of the AAEMs is a vital property to evaluate their potential application in a severe alkaline environment. Though it has been proved that an OH-concentration of 1 M is sufficient to *ex situ* elevate the alkaline stability of the AAEMs for their application in fuel cells,[23,26,32] it is still necessary to further determine the alkaline stability of the AAEMs in the severe alkaline condition. Therefore, a higher concentration alkaline solution (2.5 M KOH) was used in this work to investigate the alkaline stability of the QA-SEBS$_x$-*g*-PEG$_y$-*M*. The changes of ion conductivity, IEC, in-plane dimensions and mechanical properties of the membranes before and after being treated in 2.5 KOH at 60 °C are used to estimate the alkaline stability of these AAEMs. From Fig. S2† and 6, it can be found that the conductivity, IEC and mechanical property values of the PEG-grafted membrane remained almost unchanged in 1 M and 2.5 M KOH (this concentration is rarely used in the literature to confirm the alkaline stability of AAEMs) at 60 °C. This AAEM would swell in

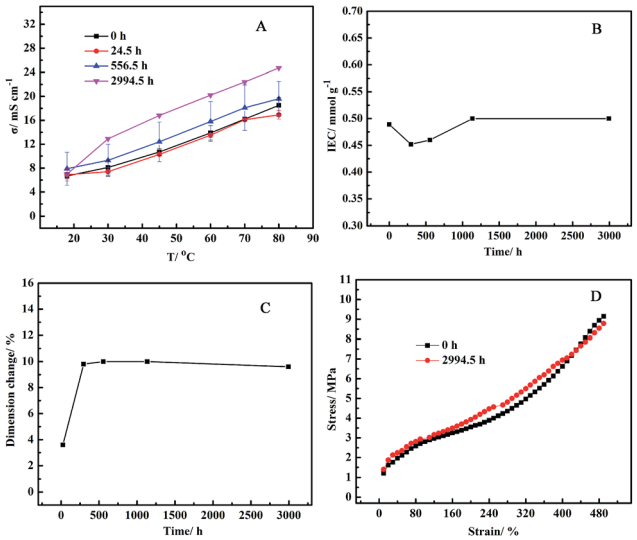

Fig. 6 Changes of conductivity, IEC, dimensions and mechanical properties of QA-SEBS$_{0.15}$-*g*-PEG$_{0.1}$-1000 after exposure to 2.5 M KOH at 60 °C for different times.

2.5 M KOH at 60 °C over 300 h and then remain stable in this environment. From the test results, it can be concluded that the main chain and the functional groups of the QA-SEBS$_x$-*g*-PEG$_y$-*M* AAEMs are stable enough in 2.5 M KOH at 60 °C for about 3000 h, which is equal to even better than that of the other AAEMs in refs. 15, 29 and 33 (Table S1†).

Performance of the fuel cell using SEBS-based AAEM

The SEBS-based AAEMs show very good physicochemical properties, such as high conductivity, mechanical and chemical stability, and so the QA-SEBS$_{0.2}$-*g*-PEG$_0$-*M* membrane was used to fabricate a membrane electrode assembly (MEA). Fig. 7 shows the polarization and power density curves of the alkaline anion exchange membrane fuel cell (AAEMFC) operating at 50 °C using the above MEAs. From Fig. 7, it can be seen that the open-circuit voltage and the peak power density of the fuel cell are over 1.04 V and 146 mW cm^{-2}, respectively, indicating that QA-SEBS$_{0.2}$-*g*-PEG$_0$-*M* possesses a relatively good gas-separation ability and ion-conductivity.

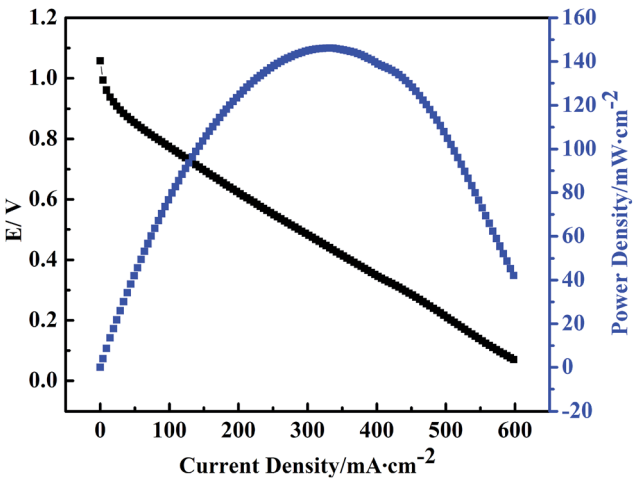

Fig. 7 Polarization and power density curves of AAEMFCs assembled using QA-SEBS$_{0.2}$ as AAEMs. The test temperature was 50 °C.

It should be also noted that the performance of the fuel cell using the SEBS-based membranes could be improved by further optimizing the electrode structure and lowering the resistance of the membranes.

Conclusions

The PEG-grafted SEBS-based AAEMs with high mechanical and chemical stability and conductivity were designed, prepared and characterized. When subjected to tensile strain, the elongation at the breaking point of SEBS-based AAEMs is 80 times greater than that of the polystyrene-based membranes. Remarkably, these AAEMs were stable enough in 2.5 M KOH at 60 °C for about 3000 h, which is rare in the recent literature. Furthermore, the properties of the membranes could be optimized by modulating the CD of SEBS, PEG molecular weight or the PEG-grafting degree. Especially, the grafting of PEG could enhance the conductivity of these AAEMs (80 °C, from 29.2 mS cm^{-1} to 51.9 mS cm^{-1}) due to the enlargement of the ion-conducting channels (as revealed by TEM). The peak power density of an H_2/O_2 single fuel cell using this SEBS-based AAEM was up to 146 mW cm^{-2} at 50 °C.

However, the relationship between the conductivity of AAEM and the size of ion-conducting channel remains unclear. The size of the hydrated OH^- is still also unclear, thus the size of the channel that would be most favorable for the conduction of OH^- in AAEM is a subject of debate. It is necessary to adequately understand the influence of the microscale structure (especially the size of the ion-conducting channels) on the properties of the AAEM, which is important for enhancing the properties of AAEM by designing the microscale-structure.

Acknowledgements

This work is financially supported by the National Basic Research Program of China (2012CB215500).

Notes and references

1 J. Pan, C. Chen, L. Zhuang and J. Lu, *Acc. Chem. Res.*, 2011, **45**, 473–481.
2 J. Pan, Y. Li, J. Han, G. Li, L. Tan, C. Chen, J. Lu and L. Zhuang, *Energy Environ. Sci.*, 2013, **6**, 2912–2915.
3 N. Li, M. D. Guiver and W. H. Binder, *ChemSusChem*, 2013, **6**, 1376–1383.
4 B. Schwenzer, J. Zhang, S. Kim, L. Li, J. Liu and Z. Yang, *ChemSusChem*, 2011, **4**, 1388–1406.
5 S. L. Mallinson, J. R. Varcoe and R. C. T. Slade, *Electrochim. Acta*, 2014, **140**, 145–151.
6 P. G. Bruce, S. A. Freunberger, L. J. Hardwick and J.-M. Tarascon, *Nat. Mater.*, 2012, **11**, 19–29.

7 D. Pletcher and X. Li, *Int. J. Hydrogen Energy*, 2011, **36**, 15089–15104.
8 Y. Leng, G. Chen, A. J. Mendoza, T. B. Tighe, M. A. Hickner and C.-Y. Wang, *J. Am. Chem. Soc.*, 2012, **134**, 9054–9057.
9 E. Guler, Y. Zhang, M. Saakes and K. Nijmeijer, *ChemSusChem*, 2012, **5**, 2262–2270.
10 H. Luo, P. Xu, P. E. Jenkins and Z. Ren, *J. Membr. Sci.*, 2012, **409–410**, 16–23.
11 J. Ran, L. Wu, Q. Ge, Y. Chen and T. Xu, *J. Membr. Sci.*, 2014, **470**, 229–236.
12 J. Pan, C. Chen, Y. Li, L. Wang, L. Tan, G. Li, X. Tang, L. Xiao, J. Lu and L. Zhuang, *Energy Environ. Sci.*, 2014, **7**, 354–360.
13 J. R. Varcoe, P. Atanassov, D. R. Dekel, A. M. Herring, M. A. Hickner, P. A. Kohl, A. R. Kucernak, W. E. Mustain, K. Nijmeijer, K. Scott, T. Xu and L. Zhuang, *Energy Environ. Sci.*, 2014, **7**, 3135–3191.
14 B. Lin, H. Dong, Y. Li, Z. Si, F. Gu and F. Yan, *Chem. Mater.*, 2013, **25**, 1858–1867.
15 J. Han, Q. Liu, X. Li, J. Pan, L. Wei, Y. Wu, H. Peng, Y. Wang, G. Li, C. Chen, L. Xiao, J. Lu and L. Zhuang, *ACS Appl. Mater. Interfaces*, 2015, **7**, 2809–2816.
16 X. Wang, M. Li, B. T. Golding, M. Sadeghi, Y. Cao, E. H. Yu and K. Scott, *Int. J. Hydrogen Energy*, 2011, **36**, 10022–10026.
17 G. Merle, M. Wessling and K. Nijmeijer, *J. Membr. Sci.*, 2011, **377**, 1–35.
18 O. M. M. Page, S. D. Poynton, S. Murphy, A. Lien Ong, D. M. Hillman, C. A. Hancock, M. G. Hale, D. C. Apperley and J. R. Varcoe, *RSC Adv.*, 2013, **3**, 579–587.
19 Z. Si, L. Qiu, H. Dong, F. Gu, Y. Li and F. Yan, *ACS Appl. Mater. Interfaces*, 2014, **6**, 4346–4355.
20 O. D. Thomas, K. J. W. Y. Soo, T. J. Peckham, M. P. Kulkarni and S. Holdcroft, *J. Am. Chem. Soc.*, 2012, **134**, 10753–10756.
21 W. Li, S. Wang, X. Zhang, W. Wang, X. Xie and P. Pei, *Int. J. Hydrogen Energy*, 2014, **39**, 13710–13717.
22 K. J. T. Noonan, K. M. Hugar, H. A. Kostalik, E. B. Lobkovsky, H. D. Abruña and G. W. Coates, *J. Am. Chem. Soc.*, 2012, **134**, 18161–18164.
23 Y. Zha, M. L. Disabb-Miller, Z. D. Johnson, M. A. Hickner and G. N. Tew, *J. Am. Chem. Soc.*, 2012, **134**, 4493–4496.
24 S. Chempath, J. M. Boncella, L. R. Pratt, N. Henson and B. S. Pivovar, *J. Phys. Chem. C*, 2010, **114**, 11977–11983.
25 F. Gu, H. Dong, Y. Li, Z. Si and F. Yan, *Macromolecules*, 2013, **47**, 208–216.
26 C. Yang, S. Wang, W. Ma, L. Jiang and G. Sun, *J. Membr. Sci.*, 2015, **487**, 12–18.
27 S. A. Nuñez and M. A. Hickner, *ACS Macro Lett.*, 2012, **2**, 49–52.
28 O. I. Deavin, S. Murphy, A. L. Ong, S. D. Poynton, R. Zeng, H. Herman and J. R. Varcoe, *Energy Environ. Sci.*, 2012, **5**, 8584–8597.
29 N. Li, Y. Leng, M. A. Hickner and C.-Y. Wang, *J. Am. Chem. Soc.*, 2013, **135**, 10124–10133.
30 C. G. Arges and V. Ramani, *Proc. Natl. Acad. Sci. U. S. A.*, 2013, **110**, 2490–2495.
31 C. G. Arges and V. Ramani, *J. Electrochem. Soc.*, 2013, **160**, F1006–F1021.
32 C. Yang, S. Wang, W. Ma, L. Jiang and G. Sun, *J. Mater. Chem. A*, 2015, **3**, 8559–8565.
33 J. Ran, L. Wu, B. Wei, Y. Chen and T. Xu, *Sci. Rep.*, 2014, **4**, 6486.